

# Multisite phosphorylation of c-Jun at threonine 91/93/95 triggers the onset of c-Jun pro-apoptotic activity in cerebellar granule neurons

CE Reddy<sup>1,4</sup>, L Albanito<sup>1,4</sup>, P De Marco<sup>2</sup>, D Aiello<sup>3</sup>, M Maggiolini<sup>2</sup>, A Napoli<sup>3</sup> and AM Musti<sup>\*,1,2</sup>

Cerebellar granule cell (CGC) apoptosis by trophic/potassium (TK) deprivation is a model of election to study the interplay of pro-apoptotic and pro-survival signaling pathways in neuronal cell death. In this model, the c-Jun N-terminal kinase (JNK) induces pro-apoptotic genes through the c-Jun/activator protein 1 (AP-1) transcription factor. On the other side, a survival pathway initiated by lithium leads to repression of pro-apoptotic c-Jun/AP-1 target genes without interfering with JNK activity. Yet, the mechanism by which lithium inhibits c-Jun activity remains to be elucidated. Here, we used this model system to study the regulation and function of site-specific c-Jun phosphorylation at the S63 and T91/T93 JNK sites in neuronal cell death. We found that TK-deprivation led to c-Jun multiphosphorylation at all three JNK sites. However, immunofluorescence analysis of c-Jun phosphorylation at single cell level revealed that the S63 site was phosphorylated in all c-Jun-expressing cells, whereas the response of T91/T93 phosphorylation was more sensitive, mirroring the switch-like apoptotic response of CGCs. Conversely, lithium prevented T91/T93 phosphorylation and cell death without affecting the S63 site, suggesting that T91/T93 phosphorylation triggers c-Jun pro-apoptotic activity. Accordingly, a c-Jun mutant lacking the T95 priming site for T91/93 phosphorylation protected CGCs from apoptosis, whereas it was able to induce neurite outgrowth in PC12 cells. Vice versa, a c-Jun mutant bearing aspartate substitution of T95 overwhelmed lithium-mediate protection of CGCs from TK-deprivation, validating that inhibition of T91/T93/T95 phosphorylation underlies the effect of lithium on cell death. Mass spectrometry analysis confirmed multiphosphorylation of c-Jun at T91/T93/T95 in cells. Moreover, JNK phosphorylated recombinant c-Jun at T91/T93 in a T95-dependent manner. On the basis of our results, we propose that T91/T93/T95 multiphosphorylation of c-Jun functions as a sensitivity amplifier of the JNK cascade, setting the threshold for c-Jun pro-apoptotic activity in neuronal cells.

*Cell Death and Disease* (2013) 4, e852; doi:10.1038/cddis.2013.381; published online 10 October 2013

**Subject Category:** Neuroscience

By forming stable homodimer or heterodimer complexes with Fos or ATF family members, c-Jun constitutes the inducible activator protein 1 (AP-1) transcription factor.<sup>1,2</sup> Genetic studies have demonstrated a crucial role for c-Jun/AP-1 in different cellular programs, as cell cycle progression, differentiation and apoptosis.<sup>3,4</sup> c-Jun transactivation is mainly regulated by the c-Jun N-terminal kinase (JNK) pathway, through phosphorylation of its N-terminal domain at S63/S73 and threonine T91/T93.<sup>5–9</sup> These two groups of phosphorylation regulate c-Jun transactivity by two distinct mechanisms. In the first mechanism, S63/S73 phosphorylation promotes the expression of c-Jun target genes by facilitating c-Jun physical interactions with the coactivator CPB/p300.<sup>10,11</sup> In the second mechanism, c-Jun phosphorylation on both S63/S73 and T91/T93 is necessary for releasing specific

c-Jun target genes from transcriptional repression.<sup>7,12,13</sup> These studies suggest that, whereas S63/S73 phosphorylation is necessary for both mechanisms of c-Jun transactivation, T91/T93 phosphorylation may act as a regulatory signal switching 'on' specific classes of c-Jun/AP-1 target genes by transcriptional derepression. In line with this hypothesis, S63/S73 phosphorylation is induced by a myriad of extracellular signals with either transient or prolonged signaling dynamics<sup>14,15</sup> and it functions in diverse physiological pathways, inducing genes involved in cell cycle progression, differentiation and apoptosis.<sup>3,4,16</sup> Differently, T91/T93 phosphorylation by JNK is induced mostly by destructive cues, including genotoxic stress and chemotherapeutic drugs.<sup>8,14,17</sup> Moreover, T91/T93 phosphorylation requires a priming event at the adjacent T95 site.<sup>8</sup> Abrogation of this priming site

<sup>1</sup>Institute for Clinical Neurobiology, University of Würzburg, Würzburg, Germany; <sup>2</sup>Department of Pharmacy, Health and Nutrition Sciences, University of Calabria, Rende, Italy and <sup>3</sup>Department of Chemistry and Chemical Technology, University of Calabria, Rende, Italy

\*Corresponding author: AM Musti, Department of Pharmacy, Health and Nutritional Sciences, University of Calabria I-87036 Rende, Italy. Tel: +39 0984493149 or Institute für Klinische Neurobiologie, University of Würzburg, Versbacher Street 5, D-97078 Würzburg, Germany. Tel: +49 (0)93120144030; Fax: +49 (0)93120144009; E-mail: E\_Musti\_A@ukw.de

<sup>4</sup>Present address: Endocrinology, Department of Health Sciences, Magna Graecia University of Catanzaro, Campus Universitario, Località Germaneto, 88100 Catanzaro, Italy

**Keywords:** c-Jun; JNK; cell death; neurons; trophic/potassium deprivation; lithium

**Abbreviations:** CGCs, cerebellar granule cell; TK, trophic/potassium; JNK, c-Jun N-terminal kinase; AP-1, activator protein 1; Puma, p53 upregulated modulator of apoptosis; Bim, Bcl2-interacting mediator of cell death; GSK3 $\beta$ , glycogen synthase kinase 3 beta; TUNEL, terminal deoxynucleotidyl transferase dUTP nick end labeling; NGF, nerve growth factor; HAP, hydroxyapatite affinity chromatography

Received 18.6.13; revised 29.7.13; accepted 05.8.13; Edited by A Verkhatsky

impairs c-Jun transactivation and lead to selective inhibition of T91/T93 phosphorylation by various types of genotoxic stress, including UV radiation and anisomycin.<sup>8</sup> Importantly, it has been shown that in mammal cells the JNK cascade converts damaging stress stimuli in a sensitive switch-like response.<sup>18</sup> Therefore, the differential regulation of the S63/S73 sites *versus* the T91/T93 may reflect a switch-like response of JNK to genotoxic cues, with small stimuli rising S63/S73 phosphorylation and larger supra-threshold stimuli inducing T91/T93 phosphorylation.

In the central nervous system, c-Jun transactivation by JNK has a crucial role in diverse cellular processes, including neuronal cell death, glial-mediated neuroinflammation and neurite outgrowth.<sup>19–21</sup> Until now, the relevance of c-Jun N-terminal phosphorylation in these processes has been examined only for the S63/S73 sites.<sup>22–24</sup> These studies have shown that S63/S73 phosphorylation is crucial for exitotoxic neuronal apoptosis<sup>22</sup> and for neuronal cell death by either trophic or tropic/potassium deprivation of sympathetic neurons and cerebellar granule cells (CGC), respectively.<sup>23,25</sup> However, S63/S73 phosphorylation is also involved in neuronal differentiation processes, as neurite outgrowth in PC12 cells<sup>26,27</sup> and neurotransmitter specification in early neuronal development.<sup>28</sup> Moreover, S63/S73 phosphorylation is required for the induction of inflammatory cytokines in immune-regulatory cells, including spinal astrocytes and Bergman glial cells.<sup>20,29,30</sup> Yet, an important question remains as how can the JNK signaling pathway act through the same transcription factor to evoke quite different cellular responses.

Here, we have investigated the function of site-specific regulation of c-Jun multiphosphorylation at the S63 and T91/T93 JNK sites in CGC apoptosis by trophic/potassium (TK)-deprivation. This model of cell death is dependent on c-Jun expression and transactivation by JNK, which in turn leads to the induction of pro-apoptotic genes, such as Puma (p53 upregulated modulator of apoptosis) and Bim (Bcl2-interacting mediator of cell death).<sup>24</sup> Conversely, CGC apoptosis by TK-deprivation is impaired by lithium, through a survival pathway involving glycogen synthase kinase 3 beta (GSK3 $\beta$ ) inhibition and the repression of pro-apoptotic c-Jun target genes, without interfering with JNK activity.<sup>31,32</sup> We provide evidence that lithium protects CGCs from TK-deprivation by inhibiting c-Jun phosphorylation at T91/T93/T95 sites. Furthermore, we show that abrogation of T91/T93/T95 phosphorylation has no consequence on the capacity of c-Jun to induce neurite outgrowth in PC12 cells, suggesting that site-specific regulation of c-Jun phosphorylation is one

possible mechanism underlying the functional dichotomy of the JNK/c-Jun pathway in the brain.

## Results

**Phosphorylation of c-Jun N-terminal domain in cerebellar granule neurons.** To investigate the role of c-Jun phosphorylation at T91/T93 in neuronal death, we set up a previously described experimental system consisting of primary cultures of mouse CGCs undergoing cell death in response to TK-deprivation.<sup>24</sup> P7 mouse cerebella were used to generate CGCs, which were cultured for 7 days (DV7) in presence of serum and high potassium concentration (25 mM); CGC culture were then switched to low potassium concentration (5 mM) for further 18 h. Cell death of CGCs was assessed at single cell level by examining the nuclear morphology of DAPI-stained nuclei using immunofluorescence microscopy. It is worth noting that in our experimental settings (see Supplementary Figure 1) 100% of DAPI-stained condensed nuclei resulted terminal deoxynucleotidyl transferase dUTP nick end labeling (TUNEL)-positive, confirming that morphological analysis of DAPI-stained nuclei is a valuable assay to detect apoptosis. In line with previous studies<sup>31,32</sup> we found that ~55% of cells presented condensed nuclei in TK-deprived CGC cultures, whereas the JNK-specific inhibitor SP100125 (SP) and lithium reduced the frequency of condensed nuclei to 8% and 18%, respectively (Figure 1a).

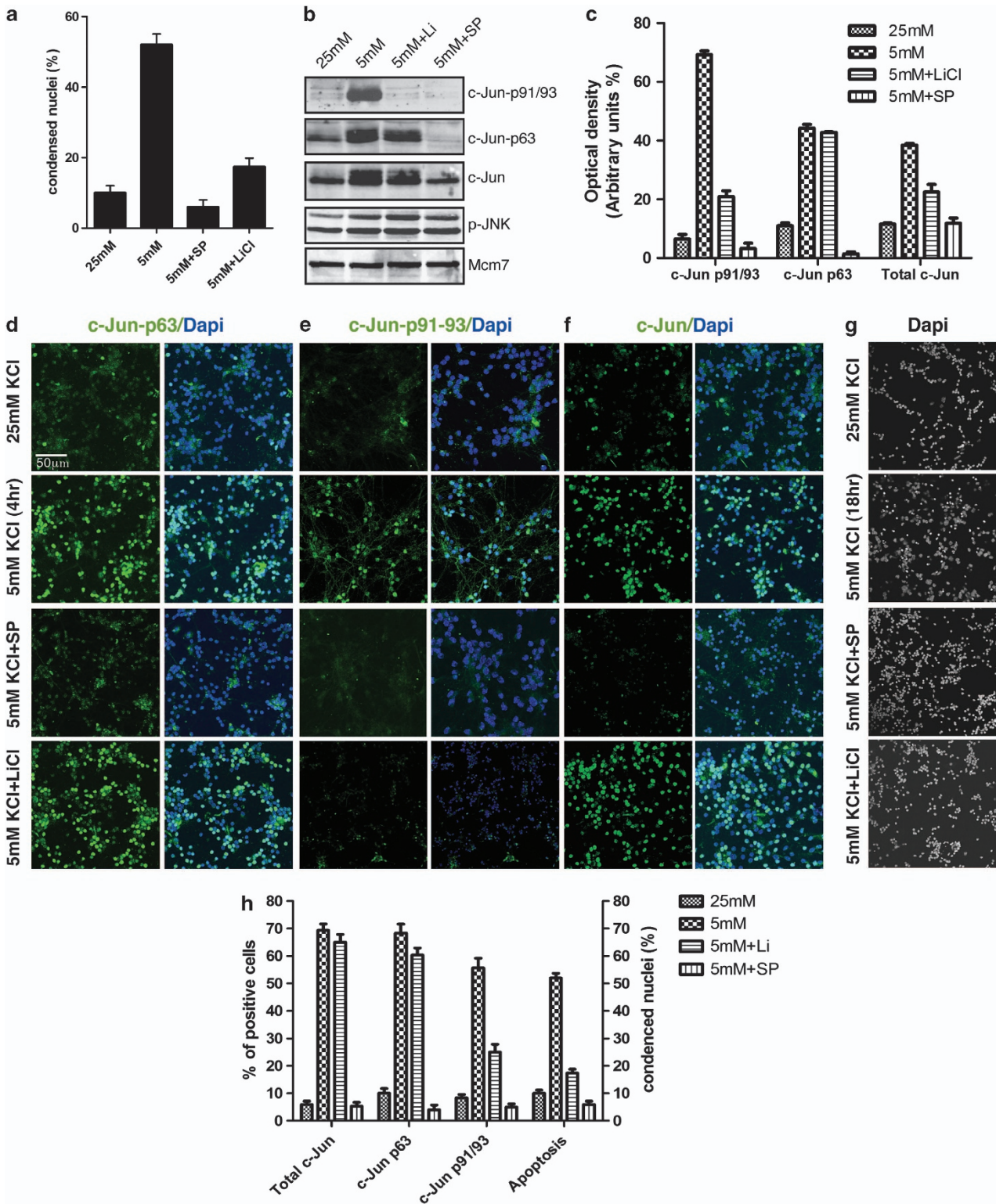
Next, we investigated site-specific c-Jun N-terminal phosphorylation by TK-deprivation, using site-specific c-Jun antibodies recognizing c-Jun when phosphorylated at S63 (c-Jun-p63) or at T91/T93 (c-Jun-p91/93). c-Jun phosphorylation was evaluated at 4 h after TK-deprivation, as maximal c-Jun phosphorylation by TK was reported to arise at this time period.<sup>33</sup> We found that TK-deprivation induced c-Jun protein levels and c-Jun phosphorylation at both S63 and T91/T93 in a SP-sensitive manner (Figure 1b and c). This finding is in agreement with previous studies demonstrating that both c-Jun expression and N-terminal phosphorylation are dependent on JNK activity.<sup>1,4,14</sup> In contrast, lithium significantly impaired T91/T93 phosphorylation, whereas had no effects on S63 phosphorylation or JNK activation.

The pattern of S63 and T91/93 phosphorylation was then confirmed at single cell level. To this aim, we used site-specific c-Jun phospho-antibodies or total c-Jun antibodies to perform immunofluorescence analysis of c-Jun phosphorylation after 4 h of TK-deprivation (Figure 1d–f). In addition, parallel CGC

**Figure 1** c-Jun N-terminal phosphorylation in cerebellar granule neurons. (a) CGCs were cultured in 25 mM K and then switched to 5 mM K medium for 18 h, either in absence or in presence 10  $\mu$ M SP600125 (SP) or 10  $\mu$ M LiCl, as indicated. Cells were then fixed and nuclei were stained with DAPI. Condensed nuclei were counted by fluorescence microscopy. Columns indicate the average percentage number of condensed nuclei present in 10 different fields, with bars indicating S.D. (b) Western blot analysis of CGCs cultured either in 25 or 5 mM K medium for 4 h and treated with either SP600125 (10  $\mu$ M) or LiCl (10  $\mu$ M) as indicated. c-Jun N-terminal phosphorylation or phosphorylated JNK (p-JNK) were determined by using the indicated antibodies. c-Jun expression levels were measured by using a total c-Jun antibody as indicated. Protein levels were normalized by using the Mcm7 antibody. (c) Densitometric analysis of western blot analysis shown in panel c. Values are presented as optical density (OD; expressed in arbitrary units) relative to the control (Mcm7). Bars represent S.D. from three different densitometric quantification of analogous experiments shown in panel c. (d–f) Immunofluorescence analysis of CGCs cultured in 25 or 5 mM K medium for 4 h and treated with either SP600125 (10  $\mu$ M) or LiCl (10  $\mu$ M) as indicated. Cells were then fixed and nuclei were stained with DAPI; c-Jun N-terminal phosphorylation and expression were detected by immunocytochemical staining using c-Jun-p63 Ab (d), or c-Jun-pT-91/T93 (e), or c-Jun total Ab (f). (g) Immunofluorescence analysis of CGC cultures TK-deprived for 18 h and analyzed for condensed nuclei by DAPI staining. (h) Quantification of results shown in d–g. Columns indicate the average percentage number of immunoreactive cells (d–f) or condensed nuclei (g) present in 10 different fields, with bars indicating S.D.

cultures were TK-deprived for 18h and analyzed for condensed nuclei by DAPI staining (Figure 1g). As shown in Figure 1d–h, the percentage of TK-deprived cells resulting positive for either total c-Jun or c-Jun-p63 antibodies were very comparable, indicating that c-Jun was phosphorylated at

S63 in the vast majority of c-Jun-expressing cells (70% of total cells). On the other hand, the percentage of cells positive for c-Jun-p91/93 was circa 55% of total TK-deprived cells, indicating that extensive N-terminal phosphorylation at both S63 and T91/T93 is present only in a subpopulation of





c-Jun-expressing cells. This finding suggests that TK-deprivation differentially regulates S63 and T91/T93 phosphorylation of c-Jun, with the T91/T93 sites responding in a sensitive fashion and mirroring the switch-like apoptotic response of TK-treated CGCs (compare the percentage of apoptotic cells with that of T91/T93-positive cells).

**Lack of T91/93 phosphorylation impairs apoptosis but not neurite outgrowth.** As c-Jun phosphorylation at T91–93 is dependent on the T95 priming site,<sup>8</sup> we then validated the role of the T91/T93 sites in neuronal cell death. To this aim, we analyzed a c-Jun mutant bearing alanine substitution of T95 (c-JunA95). We used a lentiviral approach to reintroduce the expression of either influenza-hemagglutinin (HA)-tagged c-Jun-wt or c-JunA95 proteins in primary CGCs cultures generated from conditional KO mice lacking c-Jun expression in the CNS (c-Jun  $\Delta$ N mice).<sup>34</sup> As the percentage of lentiviral-infected cells was circa 70% of total cells, we used the non-infected cells as internal control.

As expected from previous studies, we found that the rate of TK-induced apoptosis resulted reduced in CGCs generated from Jun $\Delta$ N mice (19 *versus* 60% of c-Jun-expressing CGCs) (Figure 2c). In contrast, TK-deprivation efficiently induced cell death in CGCs expressing c-Jun-wt proteins. In contrast, cell death was impaired in CGCs expressing the c-JunA95 mutant. These results indicate that reintroduction of c-Jun-wt expression, but not that of the c-JunA95 mutant, restores the standard rate of CGC apoptosis by TK-deprivation in c-Jun $\Delta$ N mice. Notably, c-Jun-wt was fully phosphorylated at both S63 and T91/T93 in response to TK-deprivation, whereas N-terminal phosphorylation of c-JunA95 was restricted to S63 (Figure 2d), confirming the crucial role of the T95 site in priming T91/T93 phosphorylation by TK-deprivation.

As c-Jun is a transcriptional factor, we next evaluated whether the inability of the c-JunA95-HA mutant to rescue apoptosis was coupled to the lack of c-Jun transactivity. To this aim, we performed reporter gene assays using a

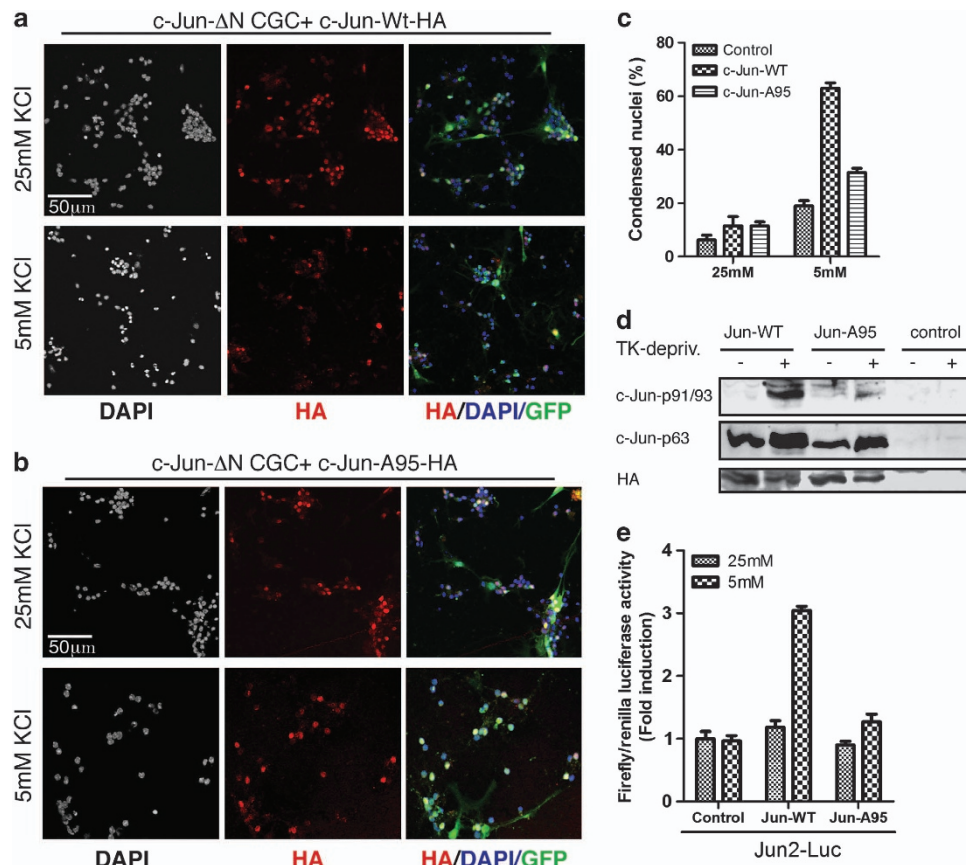


**Figure 2** Lack of T91/93 phosphorylation protects from cell death. (a and b) Confocal analysis of CGCs generated from c-Jun- $\Delta$ N mice and infected with GFP-tagged lentivirus particles expressing either HA-tagged c-Jun proteins: c-Jun-wt-HA (a) or c-JunA95-HA (b). After infections, cells were cultured for 6 days and then treated as indicated for 18 h. After fixation, nuclei were stained by DAPI and immunostained with HA antibody. (c) Quantification of results shown in a and b. Columns indicate the average percentage number of condensed nuclei present in 10 different fields, with bars indicating S.D. (d) Western blot analysis of CGCs from c-Jun- $\Delta$ N mice infected with lentivirus as described in a and b. After infection, cells were cultured either in 25 mM K or shifted to 5 mM K medium for 4 h, as indicated. Control represents not infected CGCs. c-Jun N-terminal phosphorylation was determined by using the indicated c-Jun phospho-specific antibodies. The levels of c-Jun-HA proteins were determined by using the HA antibody. (e) CGCs from c-Jun- $\Delta$ N mice were transfected with Jun2-luc reporter plasmids in combination with plasmids expressing either c-Jun-wt-HA or c-JunA95-HA proteins or empty vector (indicated as control). After infection, cells were cultured either in 25 mM K or shifted to 5 mM K medium for 4 h, as indicated. The luciferase activities were normalized to the internal transfection control. Values of CGCs transfected with empty vectors and cultured in 25 mM K were set as onefold induction. Bar graphs represent the mean  $\pm$  S.D. of three independent assays

Jun2-luciferase (Jun2-luc) reporter, previously shown to be induced by TK-deprivation in CGCs.<sup>25</sup> The Jun2-luc reporter was transfected in CGCs generated from c-Jun $\Delta$ N mice, either alone or together with expression vectors expressing either c-Jun-wt-HA or c-JunA95-HA proteins. As expected, the c-Jun2-luc reporter was not induced by TK-deprivation in CGCs from c-Jun $\Delta$ N mice. Conversely, reintroduction of c-Jun-wt-HA caused approximately a threefold increase of luciferase activity in response to TK-deprivation, whereas c-JunA95-HA had a very limited effect. Notably, the western analysis shown in Figure 2d indicates that c-Jun-wt-HA and c-JunA95-HA proteins have equal steady-state expression levels in CGCs. Taken together, these results suggest that lack of c-Jun phosphorylation at the T91/T93/T95 sites impairs the induction of c-Jun transactivity by TK-deprivation and in turn protects from cell death.

Next, we investigated the capability of the c-JunA95 mutant to induce neurite outgrowth in PC12 cells cultured in absence of nerve growth factor (NGF), a well described process that is induced by ectopic expression of c-Jun and depend on S63/S73 phosphorylation<sup>26,27</sup> As shown in Figure 3, c-Jun-wt and c-JunA95 were equally able to induce neurite outgrowth in naïve PC12 cells. These results exclude that the effect of the c-JunA95 mutant on cell death was secondary to a defect altering c-Jun transactivity independently of T91/T93 phosphorylation. In addition, they establish that c-Jun multiphosphorylation on T91/T93/T95 is required for neuronal cell death of CGCs, whereas it has no roles in Jun-dependent neurite outgrowth in naïve PC12 cells.

**Deregulation of c-Jun phosphorylation at the T91/T93 sites recovers apoptosis in presence of lithium.** Next, we assessed whether lithium protect CGCs from TK-deprivation by inhibiting the priming event preceding T91/T93 phosphorylation. To assess this hypothesis, we used a c-Jun mutant bearing aspartate substitution of T95 (c-JunD95), which was previously shown to acquire the same kinetic of S63/S73 phosphorylation in response to JNK activation.<sup>8</sup>

As shown in Figure 4, we found that lithium impaired TK-deprivation-induced apoptosis in CGCs generated from c-Jun $\Delta$ N mice and expressing c-Jun-wt proteins (Figure 4a), whereas it had a poor protective effect in CGCs expressing c-JunD95-mutated proteins (Figure 4b). However, the JNK inhibitor SP100125 efficiently inhibited TK-induced apoptosis in both circumstances, excluding that the c-JunD95 mutant acts independently from JNK transactivation (Figure 4a–c). These results suggest that inhibition of T91/93/95 phosphorylation underlies the effect of lithium on cell death.

**The T95 site of c-Jun is phosphorylated *in vivo*.** Our results suggest that lithium controls c-Jun pro-apoptotic activity by regulating the priming event preceding T91/93 phosphorylation. Most probably, this priming event consists in phosphorylation of the T95 sites, as suggested by the finding that the c-JunD95 overcomes the effect of lithium on cell death. To exclude that a different post-translational modification of T95 primes T91/93 phosphorylation, we validated that T95 is phosphorylated in cells. To this aim, we used mass spectrometry methodologies<sup>35,36</sup> to identify

N-terminal phosphopeptides of c-Jun proteins ectopically expressed in HEK-T 293 cells. First, we performed analytical experiments to analyze c-Jun phosphorylation in HEK-T 293 cells. HEK-T 293 cells were transfected with a vector expressing human c-Jun and then treated with anisomycin, a strong activator of JNKs. c-Jun resulted fully phosphorylated on both S63 and T91/T93, either before or after anisomycin treatments (Figure 5a), owing to the constitutive activation of JNKs in this cell line.<sup>37</sup> However, c-Jun phosphorylation at T91/T93 was dependent on the priming event at T95, as the c-JunA95 mutant resulted phosphorylated only at the S63 site (Figure 5b). Next, c-Jun-wt proteins were immunoprecipitated from transfected cells and immunocomplexes were processed for MALDI MS and MS/MS. In parallel, immunocomplexes were analyzed by western analysis to confirm the presence of phosphorylated T91/T93 residues (Figure 5b).

Following in-gel digestion of c-Jun immunocomplexes with proteinase K (PK), the fraction of phosphopeptides was enriched by hydroxyapatite affinity chromatography (HAP) and analyzed by MALDI MS and MS/MS. All identified phosphopeptides are listed in Table 1. In-gel PK digestion of c-Jun immunocomplexes generated three major multiphosphorylated peptides. In particular, three different triphosphorylated peptides were identified as residues 80–97, 82–97 and 89–98. The CID spectrum of segment 82–97 ( $m/z$  1956.73) is given in Figure 5c. For this segment, the MS/MS spectrum showed b ( $b\text{-H}_3\text{PO}_4$ ) and y ( $y\text{-H}_3\text{PO}_4$ ) ion series, allowing the assignment of either peptide sequence and phosphorylation sites at the T91, T93 and T95 residues. All the b-series fragments down to  $b_{10}$  ( $m/z$  1107.7) showed the ability to lose  $\text{H}_3\text{PO}_4$  (–98 Da), whereas the  $b_9$  ( $m/z$  926.7) fragment was present only in a non-phosphorylated state, indicating that the ninth residue from the N-terminus (T91) is phosphorylated. In addition, the mass difference between the  $b_{10}$  ( $m/z$  1107.7) and  $b_9$  ( $m/z$  926.7) ions is consistent with the mass of a phosphothreonine residue (181 Da). Furthermore, the presence of the ion peak  $b_{14-98}$  ( $m/z$  1566.0) and of the unmodified counterpart  $y_2$  ( $m/z$  294.2) is consistent with a phosphorylated T95 residue. The presence of T95 phosphorylation is also reliable with the mass difference between the  $y_2$  ( $m/z$  294.2) and  $y_3$  ( $m/z$  475.1) ions (181 Da). Accordingly, T93 phosphorylation was assigned by considering the mass difference between the  $y_{5-98}$  ( $m/z$  655.4) and  $y_{4-98}$  ( $m/z$  474.4) ions, as it was consistent with the mass of a phosphothreonine residue (181 Da). In a similar fashion, both phosphopeptides 80–97 and 89–98 resulted to be phosphorylated on T91, T93 and T95. A similar set of b ( $b\text{-H}_3\text{PO}_4$ ) and y ( $y\text{-H}_3\text{PO}_4$ ) ions was observed for both the doubly phosphorylated peptide (83–93) of  $m/z$  1473.58, and the mono-phosphorylated peptide (82–97) of  $m/z$  1796.80, allowing the assignment of T91–T93 and T91 phosphorylations, respectively (see Supplementary Figures 2 and 3). Figure 5d shows the MS/MS spectrum for the precursor ion of  $m/z$  1144.57 of sequence TpSDVGLLK. Interpretation of the MS/MS spectrum was straightforward because a complete b ( $b\text{-H}_3\text{PO}_4$ ) and y ion series was identified, with the  $b_{2-98}$  fragment indicating that phosphorylation occurred at the second residue from the N-terminus. This phosphorylation site was unambiguously assigned to S63.

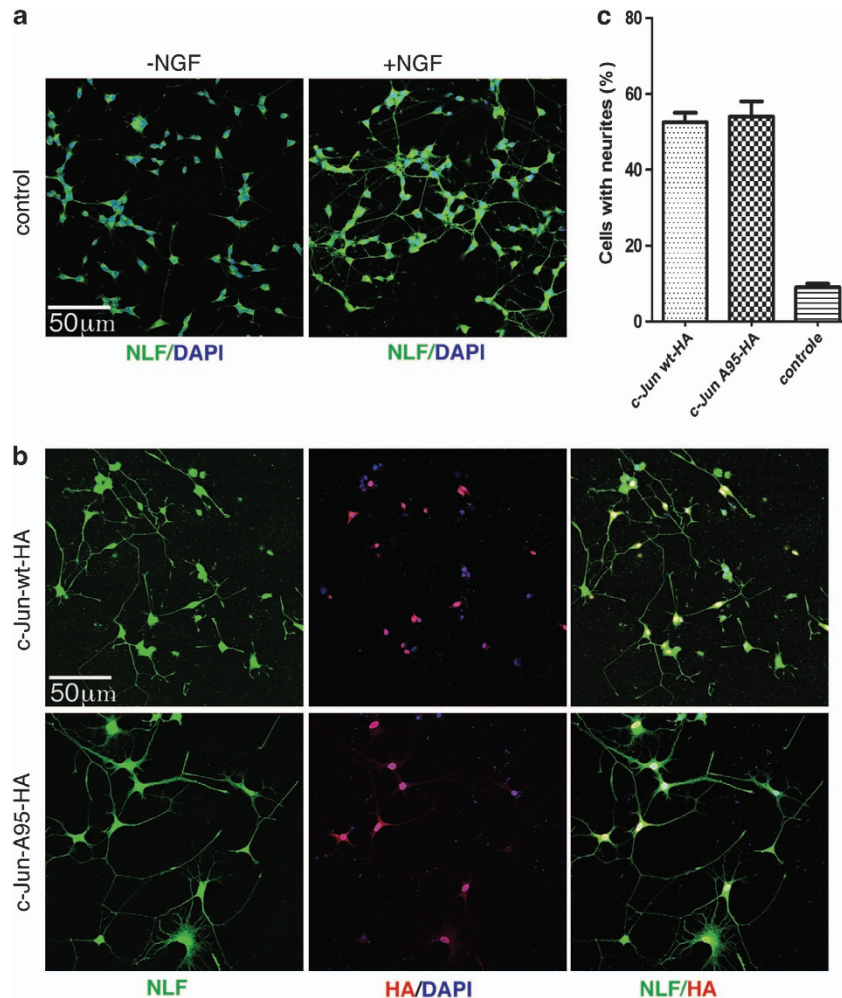


**Figure 3** Lack of T91/93 phosphorylation does not impair neurite outgrowth. (a) Confocal analysis of PC12 cells were cultured either in absence or in presence of NFG (72 h) as indicated. After fixation, cells were immunostained with neurofilament (NLF, green) antibodies. Nuclei were stained with DAPI (b) Naive PC12 cells were transfected with DNA constructs expressing either HA-tagged c-Jun-wt or Ha-tagged c-JunA95 constructs, as indicated. Transfected cells were cultured in absence of NGF for 72 h; after fixation cells were incubated with either HA (red) or NLF, green antibodies. (c) Columns indicates the average percentage number of PC12 cells with neurites present in 10 different fields, with bars indicating S.D.

Similarly, phosphopeptides 56–69 and 61–68 resulted to be phosphorylated at S63.

**JNK-1 phosphorylates T91/93 residues of recombinant c-Jun proteins *in vitro*.** Having shown that T95 is phosphorylated *in vivo*, we then asked whether the T95 site could be directly phosphorylated *in vitro* by JNK or by the lithium-sensitive kinase GSK3 $\beta$ . To this end, we transfected NSC-34 cells with plasmids expressing either c-Jun-wt-HA or c-JunA95-HA-tagged proteins and performed *in vitro* phosphorylation of immunoprecipitated c-Jun-HA proteins by using HA antibodies. c-Jun-HA immunocomplexes were then used as substrates for *in vitro* phosphorylation assays by using recombinant JNK-1, either alone or in combination with recombinant GSK3 $\beta$ . Given that T91/T93 phosphorylation is strictly dependent on the priming phosphorylation event at the T95 site, we assumed that the phosphorylation status of T91/T93 could indirectly monitor the capacity of either JNK or GSK3 $\beta$  to phosphorylate T95. Therefore, products of *in vitro* phosphorylation reactions were analyzed

by western blot using phospho-specific antibodies for either p-T91/T93 or for p-S63. As western analysis of NSC-34 total extracts revealed that Jun-HA proteins have quite low basal phosphorylation levels of the T239 GSK3 $\beta$  site but fairly good levels of the T243 priming site for T239 phosphorylation (Figure 6a), we also monitored the phosphorylation status of the T239 by using a p-T239 phospho-specific antibody. As shown in the new Figure 6b, recombinant JNK-1 was fully able to phosphorylate immunoprecipitated c-Jun-wt-HA at both S63 and T91/93 sites, whereas JNK-1 phosphorylated immunoprecipitated c-JunA95-Ha proteins only at the S63 site. In contrast, recombinant GSK3 $\beta$  had no effect of either S63 or T91/93 but it was fully able to phosphorylate both forms of c-Jun-HA proteins at the T239 site. It is worth to note that the mobility shift of c-Jun-HA proteins detected by HA-Ab (in the samples incubated with JNK-1) is due to S63 phosphorylation and therefore is observed in both c-Jun-wt-Ha and c-Jun-A95-HA proteins.

To rule out that T95 phosphorylation of c-Jun-HA immunocomplexes was achieved by a c-Jun-interacting kinase



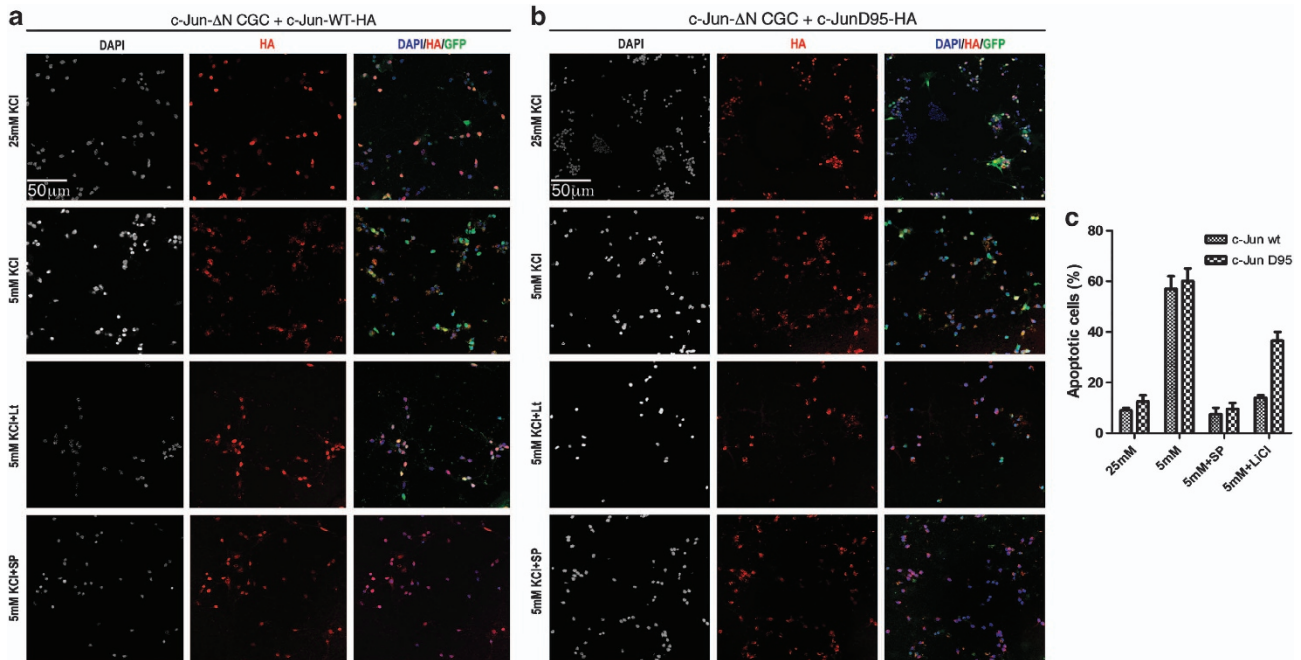


**Figure 4** Deregulation of T91/T93 phosphorylation recovers cell death in presence of lithium. **(a and b)** Confocal analysis of CGCs generated from c-Jun  $\Delta N$  mice and infected with GFP-tagged lentivirus particles expressing c-Jun-wt-HA **(a)** or Ha-c-JunD95-HA proteins **(b)**. After transduction, cells were cultured for 6 days and then treated as indicated with 25 or 5 mM K for 18 h, with or without SP600125 (10  $\mu$ M) or LiCl (10  $\mu$ M) as indicated. After fixation, nuclei were stained by DAPI and immunostained with HA antibody (red). **(c)** Quantification of results shown in **a** and **b**. Columns indicate the average percentage number of condensed nuclei present in 10 different fields, with bars indicating S.D.

different from JNK, we then performed *in vitro* phosphorylation of FL-c-Jun recombinant protein. As shown in the new Figure 6c, we found that recombinant JNK-1 was able to phosphorylate recombinant FL-c-Jun at both the S63 and T91/93 sites. All together these experiments indicate that JNK-1 is able to directly phosphorylate c-Jun at the canonical JNK T91/T93 sites and at the non-canonical T95 site. However, we cannot exclude that *in vivo* a lithium-sensitive kinase, different from GSK3 $\beta$ , is the main kinase phosphorylating the priming T95 site.

## Discussion

Gene expression by the JNK/c-Jun pathway is involved in very different cellular programs, including cell cycle progression, differentiation and apoptosis. In turn, deregulation of the JNKs/c-Jun pathway may give rise to pathological conditions, including tumor progression, neuroinflammation and degenerative loss of neurons.<sup>8,38</sup> The challenging question is how can the same signaling pathway regulate the expression of genes involved in quite different cellular programs. One level of regulation is certainly represented by the type of c-Jun partner forming the dimeric AP-1 transcription factor, which in turn binds and transactivates subsets of target genes.<sup>1,25</sup> A second level of regulation is generated by the kinetic of the JNK/c-Jun signaling pathway. Several studies have shown that depending on the kinetic of JNK activation, variations in c-Jun levels and activation periods are coupled to different patterns of gene expression.<sup>39–41</sup> Here, we propose that depending on the complexity of external signals and their

interplay with intrinsic cues, c-Jun multiphosphorylation by JNK may result differential at a site-specific level and in turn elicit different physiological responses. In particular, we provide evidence that in CGCs, apoptotic cues lead to extensive multiphosphorylation of c-Jun N-terminal domain, with T91/T93 phosphorylation setting the threshold for c-Jun pro-apoptotic activity. In contrast, a concomitant activation of survival pathways initiated by lithium inhibits T91/T93 phosphorylation with no effects on S63 phosphorylation, hence preventing the onset of c-Jun pro-apoptotic activity without interfering with possible non-destructive functions of c-Jun requiring S63 phosphorylation.

Two lines of evidence indicate that T91/T93 phosphorylation results in a threshold for c-Jun pro-apoptotic activity. The first evidence addresses the type of response of T91/T93 phosphorylation to apoptotic cues and comes from immunofluorescence analysis of c-Jun site-specific phosphorylation. This analysis shows that the response of T91/T93 phosphorylation to TK-deprivation is not graded but rather sensitive and mirrors the switch-like apoptotic response of TK-deprived neurons. The second evidence addresses the functional role of T91/T93 phosphorylation in triggering c-Jun pro-apoptotic activity and comes from the functional analysis of the c-JunA95 mutant in CGC apoptosis. This analysis shows that c-JunA95-mutated proteins are not phosphorylated at T91/T93 in response to TK-deprivation, are unable to transactivate a c-Jun/AP-1 reporter gene and failed to promote CGC apoptosis. These findings confirm that in absence of T91/T93 phosphorylation, S63-phosphorylated c-Jun is not able to promote cell death. In addition, they

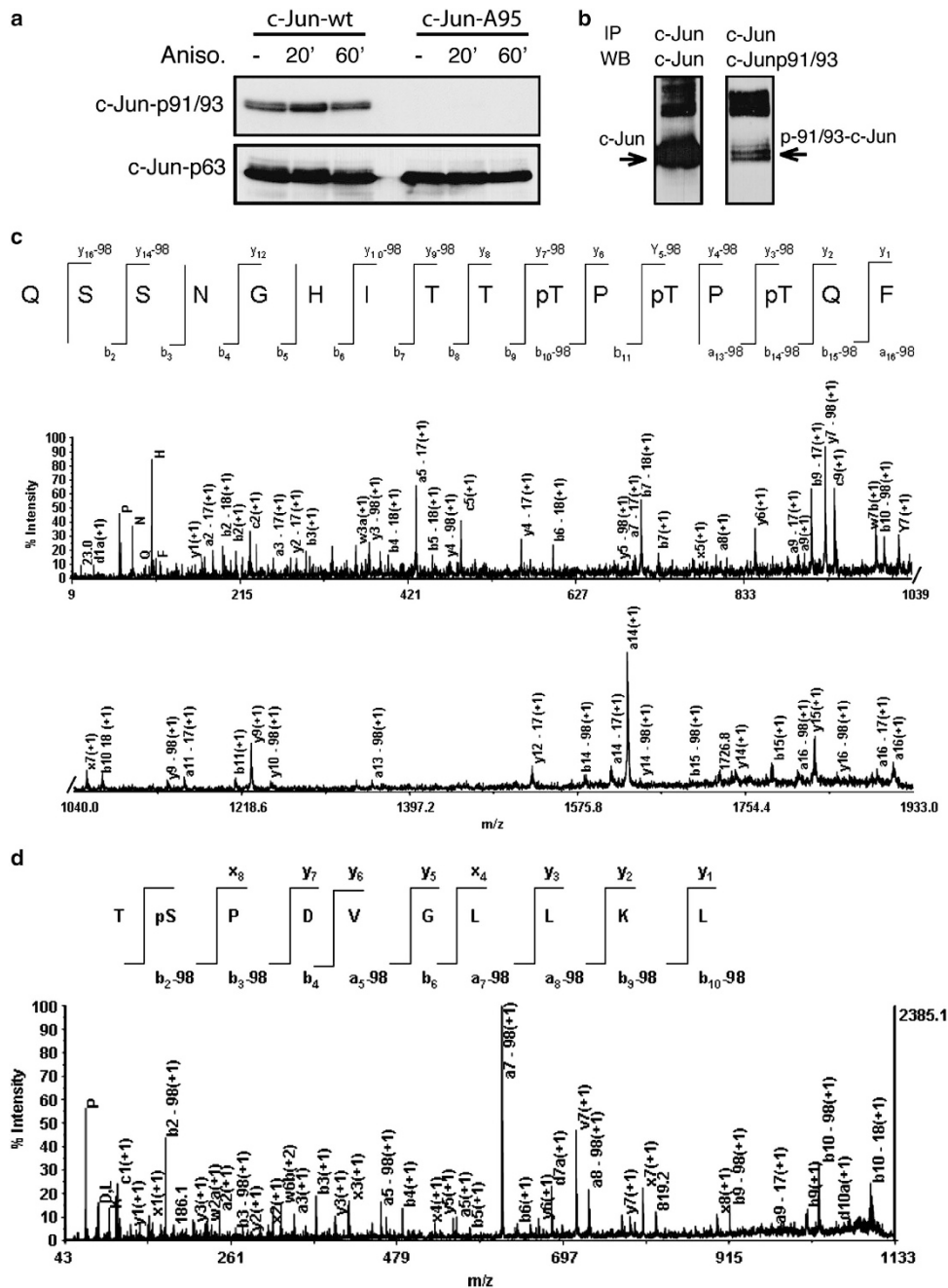


**Figure 5** Phosphorylation of amino-acid residues within c-Jun N-terminal domain. (a) Western blot analysis of HEK-293 cells transfected with DNA constructs expressing either HA-tagged c-Jun-wt or Ha-tagged c-JunA95, as indicated. After transfection, cells were treated either without or with Anisomycin (100 ng/ml) for indicated time-periods. c-Jun N-terminal phosphorylation was determined by using the indicated antibodies. (b) Lysates from anisomycin-treated c-Jun-wt-transfected HEK-T cells were immunoprecipitated using the c-total c-Jun antibody, then aliquots from c-Jun immunocomplexes were analyzed by western blot using either c-Jun total antibodies (left panel) or c-Jun-p91/93 antibodies (right panel). (c) MALDI MS/MS spectra of the  $[M + H]^+$  from segments 82–97 carrying three phosphate groups at T91, T93 and T95. (d) MALDI MS/MS spectra of the  $[M + Na]^+$  from segments 62–70 carrying one phosphate group at S63. The a, b and y ions are labeled in each spectrum, as well as b or y ions corresponding to the neutral loss of phosphoric acid ( $-98$ )

corroborate the regulatory role of the T95 site in priming T91/T93 phosphorylation by JNK. Furthermore, the finding that c-JunA95 is capable to induce neurite outgrowth in naïve PC12 cells suggests that lack of T91/T93/T95 phosphorylation may not interfere with regenerative functions of c-Jun. However, whether such a functional role of c-Jun multisite phosphorylation is a general principle, or applies

to specific neuron populations, needs to be explored in future studies.

A further question addressed by our study is the mechanism through which lithium blocks c-Jun pro-apoptotic function without inhibiting JNK activity. The specific effect of lithium on T91/T93 phosphorylation, together with the evidence that the c-JunD95 mutant resumes GCG apoptosis in presence of



**Table 1** Phosphopeptides identified by MALDI MS/MS

Sequence <sup>a</sup>	Mr found <sup>b</sup>	Mr calc <sup>b</sup>
80–97 IIQSSNGHITTPpTPpTQF	2182.90	2182.89
82–97 QSSNGHITTPpTPpTQF	1956.73	1956.72
89–98 TTpTPpTPpTQF	1233.40	1232.39
83–95 SSNGHITTPpTPT	1473.58	1473.57
87–98 HITTPpTPTQFL	1436.69	1436.68
87–96 HITTPpTPTQ	1256.50	1256.50
82–97 QSSNGHITTPpTPTQF	1796.80	1976.79
81–96 IQSSNGHITTPpTPTQpyr	1745.79	1745.77
54–60 RAKNSDL	803.44	803.44
61–68 LTpSPDVGL	881.41	881.40
62–70 TpSPDVGLLK <sup>c</sup>	1144.57	1144.56
56–69 KNSDLLTpSPDVGLL <sup>c</sup>	1589.73	1589.73

<sup>a</sup>Amino-acid sequence of phosphorylated peptides identified from peptic digests on the basis of their CID spectrum. pS denotes phosphoserine and pT denotes phosphothreonine.

<sup>b</sup>All mass values are listed as monoisotopic mass.

<sup>c</sup>Denotes [M-Na]<sup>+</sup> adduct

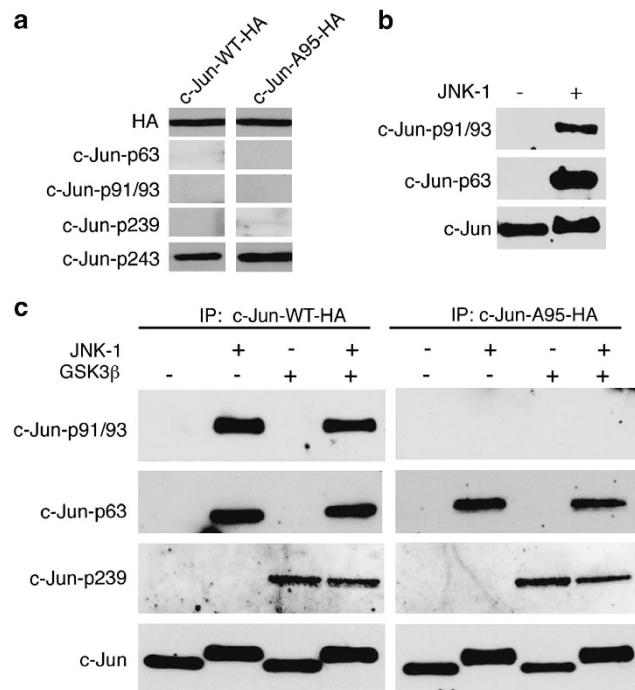


**Figure 6** JNK-1 phosphorylates *in vitro* c-Jun at T91/93 in a T95-dependent manner. (a) NSC-34 cells were transfected with plasmids expressing either c-Jun-wt-HA or c-JunA95-HA-tagged proteins (as indicated) and levels of c-Jun site-specific phosphorylation were analyzed by western blot of total extracts by using the indicated antibodies. (b) Either c-Jun-wt-HA or c-JunA95-HA-tagged proteins were immunoprecipitated by using HA antibodies, then c-Jun-HA immunocomplexes were used as substrates for *in vitro* phosphorylation assays by using recombinant JNK-1, either alone or in combination with recombinant GSK3β as indicated. Products of *in vitro* phosphorylation reactions were analyzed by western blot using c-Jun-phospho-specific antibodies for either p-T91/T93, p-S63 or p-239. Total amounts of c-Jun proteins were determined by using the c-Jun total antibody. (c) *In vitro* phosphorylation assay of recombinant FL-c-Jun protein (Ezio Life Sciences) incubated with recombinant JNK-1 as indicated. Reactions were analyzed by western blot, using either c-Jun-p91/93 or c-Jun-p-S63 phospho-specific antibodies as indicated. Total amounts of c-Jun proteins were determined by using the c-Jun total antibody

lithium, is consistent with a model whereby lithium blocks c-Jun pro-apoptotic activity by targeting the priming T95 phosphorylation event for T91/T93 phosphorylation. In such a scenario, the priming event for T91/T93 phosphorylation

acquires a crucial role in determining the output of c-Jun biological activity in response to JNK activation. Mass spectrometry analysis confirmed that c-Jun is multi-phosphorylated *in vivo* at T91/T93/T95, hence validating that T95 phosphorylation is the priming event for T91/T93 phosphorylation.

Whether lithium controls T91/T93 phosphorylation by inhibiting a T95-specific kinase or by inducing a phosphatase remains to be elucidated. However, we show that recombinant JNK-1 fully phosphorylates c-Jun *in vitro* at the T91/T93 sites in a T95-dependent manner. These results suggest that JNK sequentially phosphorylates c-Jun at T95-T93-T91 in response to TK-deprivation, whereas lithium may induce a T95-specific phosphatase. Although the T95 site does not contain the minimal S/TP sequence for MAP kinases, it has been previously shown that both JNK-2 and JNK-1 can phosphorylate a similar site in histone H2AX.<sup>42,43</sup> Future experiments will elucidate whether *in vivo* T95 is phosphorylated by JNKs or by a lithium-sensitive kinase. Alternatively, lithium might inhibit T95 phosphorylation by affecting nuclear translocation of JNKs, hence limiting the local concentration of active JNKs necessary to phosphorylate the non-canonical T95 site. Accordingly, inhibition of JNK-2-3 nuclear translocation was described to protect from apoptosis in sympathetic neurons and CGCs<sup>44,45</sup>

Our results provide the first evidence that apoptotic and survival cues give rises to different site-specific configurations of c-Jun N-terminal multiphosphorylation, each having a different functional output in neuronal cells. Furthermore, our study suggests that inhibition of T91/T93/T95 phosphorylation represents a pharmacological tool to selectively target c-Jun-dependent degenerative pathways in the nervous system.

## Materials and Methods

**Animals.** All used mouse lines were housed in the central animal facilities of the University of Wuerzburg. The animal care and ethic committees of our institutions approved all described procedures and experiments. C57Bl/6 mice were used for generation of CGCs cultures. Mice carrying a floxed c-Jun allele (c-Jun fl)<sup>46</sup> were kindly provided by Dr. Axel Behrens from Cancer Research UK. c-Jun fl/fl were crossed with mice expressing Cre-recombinase beneath the control of Nestin promoter<sup>47</sup> and crossed again to generate c-Jun fl/fl-nestin-Cre + mice (c-Jun Dn), in which both c-Jun alleles are inactivated in cells derived from embryonic neuroepithelium, resulting in CNS-specific inactivation of c-Jun fl, as previously described.<sup>34</sup>

**Lentiviral production.** DNA vectors expressing HA-tagged human c-Jun proteins<sup>8</sup> were used as templates to amplify c-Jun coding regions that were subsequently cloned into the FUGW vector<sup>48</sup> through the BamHI-NotI. The following primers were used for c-Jun sequence amplification: forward 5'-GGATCCATGACTGCAAGATGG-3' and reverse 5'-GCGGCCGCTTATCATCTAGAC3-3'. Lentiviral particles were produced as previously described<sup>49</sup> (Bender, FL). HEK 293T cells were transfected with packaging vector pCMVΔR8.9 s, generation envelope vector pVSVG and expression plasmids FUGW-c-Jun-wt HA-IRES-eGFP or FUGW-c-Jun A95 HA-IRES-eGFP or FUGW-c-Jun D95 HA-IRES-eGFP using Lipofectamine 2000 (Invitrogen, Karlsruhe, Germany). Supernatants were collected and concentrated by ultracentrifugation. Lentiviruses were aliquoted and stored at -80 °C until use.

**Primary cultures of cerebellar granular cells.** CGC cultures were generated from either C57Bl/6 P7 mice as previously described.<sup>29</sup> Briefly, mice were deeply anesthetized and injected with saline solution to remove the blood. After the removal of meninges and choroid plexus, cerebella were trypsinized with BME media containing 1% trypsin and DNase I (2 mg/ml) for 15 min at 37 °C and

then triturated in HBSS containing 10 U/ml DNase I (Roche Diagnostics, Mannheim, Germany). Cells were centrifuged at 2000 r.p.m. for 7 min and resuspended in BME (Sigma, Mannheim, Germany) containing 4 mM glutamine, 10% fetal bovine serum, 100 U/ml Penicillin/streptomycin and 25 mM KCl (Sigma-Aldrich, Hamburg, Germany). After counting, cells were plated on precoated Poly-DL-ornithine hydrobromide (PORN-Sigma) glass coverslips ( $3.5 \times 10^6$ ) or six-well multiwell plates ( $5 \times 10^6$  density). Cultures were maintained at 37 °C, 5% CO<sub>2</sub>, and media were changed every 2 days. After 24 h in culture treat the cells with Ara-C for 1 day (Cytosine-1- $\beta$ -D-arabino-furanoside) to remove proliferating and non neuronal cells. All experiments were performed 6 days after plating (DIV6). For serum potassium withdrawal experiments cells were treated with either 5 mM KCl (LK) or with 25 mM KCl (HK) for 4 h to check phosphorylation levels on western blot or treat for 18 h for apoptotic assays.

**Cell death and survival assay.** Cell death of CGCs was assessed by examining nuclear morphology following DAPI (4',6'-diamidino-2-phenylindole hydrochloride) staining as previously described.<sup>50,51</sup> Briefly, DAPI stain (0.5  $\mu$ g/ml) was added directly to PBS or to secondary antibody and incubated for 20 min at room temperature. Cells were visualized by fluorescence microscopy (SP2 Leica fluorescent microscope, Wetzlar, Germany). A minimum of 1000 cells were analyzed per each treatment. To confirm that condensed nuclei indeed denotes apoptotic cell, we costained the DAPI with TUNEL staining (*In Situ* Cell Death Detection Kit- TMR red-Roche, Mannheim, Germany) according to manufacturer's protocol. It is worth noting that in our experimental settings, 100% of TUNEL-positive cells were stained as condensed nuclei by DAPI, indicating that this is a valuable assay to measure cell death (Supplementary Figure S1).

**PC12 cell culture and transfection.** PC12 cell line was cultured on poly-D-lysine coated dishes in media containing DMEM (Invitrogen) supplemented with 10% horse serum, 5% FCS, 2 mM glutamine and penicillin/streptomycin. Cells were grown at 37 °C in 5% CO<sub>2</sub>. For neurite outgrowth, cells were plated at a density of  $1 \times 10^6$  cells per 9 cm dish. Once cells were at 60–70%, confluent PC12 cells were treated with 50 ng/ml of NGF and maintained for 3 days.

PC12 transfections with DNA constructs expressing c-Jun proteins were performed by using Lipofectamine 2000 reagent (Invitrogen) following the manufacturer's instructions. After transfections, cells were cultured in absence of NGF for 72 h, then were fixed and processed for immunofluorescence analysis.

**Immunocytochemistry.** DIV6 cerebellar granule cultures and PC12 cells were permeabilized with a blocking solution containing 0.3% TritonX-100, 10% Goat serum, 0.1% BSA in TBS for 2 h at room temperature. Then, cells were incubated overnight at 4 °C with the following primary antibodies: anti-rabbit c-Jun (Cell Signaling, NEB, Germany, 1:200), anti-rabbit phospho-c-Jun-Ser63 (Cell Signaling 1:200), anti-rabbit phospho-c-Jun-Thr91 (Cell Signaling 1:200), anti-rabbit phospho-c-Jun-Thr93 (Cell Signaling 1:200); or Anti-mouse HA-tag (Biovision, Hannover, Germany), anti anti-mouse NFL (eBioscience, Frankfurt, Germany). After removing primary antibodies, cells were washed three times (10 min each) with TBS and then incubated in permeabilization solution with Alexa-Fluor-conjugated secondary antibodies for 2 h at room temperature. Cells were then treated with DAPI for 10 min to stain the nuclei (Sigma-Aldrich 1:8000). Finally, cells were washed three times with TBS for 10 min and one time with PBS and mounted by using Mowiol (Sigma-Aldrich). Pictures were taken with the SP2 confocal microscope from Leica. Configurations of c-Jun N-terminal phosphorylation were analyzed by immunocytochemistry 4 h after treatments by using site-specific c-Jun antibodies recognizing c-Jun when phosphorylated at either S63 or at T91/T93.

**Western blot analysis.** Total lysates were prepared from cerebellar primary cultures by using RIPA buffer (50 mM Tris-HCl, pH 7.4, 1% NP-40, 0.25% Na-deoxycholate, 150 mM NaCl and 1 mM EDTA and Protease inhibitor) and leave it on ice for 10 min then centrifuge at 1300 r.p.m. for 30 min. Take supernatant add 1X Laemmli buffer (100 mM Tris-HCl, pH 5.6, 2% w/v sodium dodecyl sulfate (SDS), 20% v/v glycerol, 4% v/v b-mercaptoethanol) and cook for 5 min at 99 °C. Proteins were electrophoresed under reducing condition on 10% polyacrylamide gel and transferred onto Hybond C nitrocellulose membrane (Amersham). The membranes were first incubated overnight at 4 °C with a rabbit anti-c-Jun (Cell Signaling 1:1000), or anti-rabbit phospho-c-Jun-Ser63 (Cell Signaling 1:1000), or a mixture of anti-rabbit phospho-c-Jun-Thr91 and anti-rabbit phospho-c-Jun-Thr93 (Cell Signaling 1:1000) and MCM7 (Santa Cruz

1:2000). Blots were then incubated with peroxidase-linked anti-rabbit (1:6000; Pierce) or anti-mouse (1:6000; Chemicon) IgG conjugates for 1 h at room temperature. Signals were detected with the ECL system (Amersham Biosciences).

**Luciferase assay.** For luciferase assays, CGCs were plated into 24-well plates with 500  $\mu$ l of regular growth medium/well and at DIV5 were transfected using calcium phosphate method as previously described.<sup>33</sup> In brief, transfection solutions contained 87.6  $\mu$ l of HBS HEPES-buffered saline and 4.4  $\mu$ l of 2.5 M calcium chloride with 1.0  $\mu$ g of either c-Jun-Wt or c-Jun-A95, 250 ng of Jun2 Luc and 20 ng of Renilla plasmids. Thirty-five microliters of transfection solutions was added to a total of 500  $\mu$ l of HBSS and added to cells. Precipitation was allowed for 50 min. Then cells were washed with HBSS medium twice and incubated with condition medium. Luciferase activity was then measured using the Dual Luciferase Kit (Promega, Mannheim, Germany) according to the manufacturer's recommendations. Firefly luciferase activity was normalized to the internal transfection control provided by the Renilla luciferase activity. The normalized relative light unit values obtained from cells transfected with empty vectors and cultured at 25 mM K were set as onefold induction.

**Immunoprecipitation.** HEK 293T or NSC-34 cells were plated at density of 5 million ( $5 \times 10^6$ ) cells per 10 cm dish and 18 h later were transfected by using Lipofectamine 2000 reagent (Invitrogen) with FUGW-c-Jun constructs. After 48 hours total proteins were extracted with RIPA buffer as previously described.<sup>8</sup> Primary antibodies, either anti-rabbit c-Jun antibodies (Cell Signaling 9165) or sepharose-conjugated mouse HA antibodies (Covance clone 16B12 monoclonal), were added to total cell extracts and incubated overnight at 4 °C. Immunoprecipitated proteins complexes were collected by using Protein A-agarose beads (Roche) previously washed with PBS and equilibrated with RIPA buffer. After 1 h incubation, pellets were collected by centrifugation at 1000 g, and beads were washed three times with RIPA buffer. For *in vitro* phosphorylation assays, immunocomplexes were equilibrated in kinase buffer.

**In vitro kinase assay.** Kinase assays were performed by using either c-Jun-Ha immunocomplexes or recombinant FL-c-Jun protein (200 ng, Enzo Life Sciences, Lausen, Switzerland) and either active recombinant JNK-1 (Millipore (Zug, Switzerland) 20 ng/20  $\mu$ l reaction) or GSK3 $\beta$  (Biovision, 5 ng/20  $\mu$ l). Assays were performed in a total volume of 20  $\mu$ l, containing 1x kinase buffer (50 mM HEPES (pH 7.4), 1 mM MgCl<sub>2</sub>, 20 mM beta-glycerophosphate, 1 mM Na3VO<sub>4</sub>, 0.2 mM dithiothreitol (DTT), 1  $\mu$ M pepstatin A, 1 mM PMSF, protease inhibitor and 10 mM ATP). Reactions were stopped by the addition of SDS sample buffer (100 mM Tris (pH 6.8), 2% SDS, 10% glycerol, 5% beta-mercaptoethanol and 0.25% bromophenol blue). Phosphorylation of c-Jun proteins was analyzed by western blot analysis using either p-S63 or the p-T91/93 phospho-specific c-Jun antibodies described above.

#### Mass spectrometry and protein identification

**Materials:** Solvents (CH<sub>3</sub>OH, CH<sub>3</sub>CN and H<sub>2</sub>O, HPLC grade), reagent (CH<sub>2</sub>COONa, KCl, EDTA, pure g99.5%), trifluoroacetic acid (HPLC grade, pure g99.0%), pepsin and 3,5-dimethoxy-4-hydroxycinnamic acid (pure g99.0%), R-cyano-4-hydroxy-trans-cinnamic acid (R-CHCA, pure g99.0%) were purchased from Sigma-Aldrich Fluka (Milano, Italy). HAP (BIO-GEL HTP) was purchased from Bio-Rad (Milan, Italy).

**In-gel digestion.** For MS analysis, the spots of interest were excised from 1-DE gels and analyzed by matrix-assisted laser desorption ionization/time-of-flight (MALDI-TOF/TOF). After SDS-PAGE, discrete band was excised from the blue-coomassie-stained gel. The in-gel digestion with proteinase K was carried out as previously described.<sup>52</sup> To obtain extensively cleaved protein, the digestion was performed at 37 °C for 18 h twice. Peptides were subsequently extracted twice with 100  $\mu$ l of 50% ACN/2% trifluoroacetic acid (TFA); the extracted solutions were then combined and dried with the Speed Vac concentrator. The peptide pellets were then resuspended in 100  $\mu$ l of 40% ACN/0.1%. For MS MS/MS experiments, the peptic peptide mixture (10  $\mu$ l) was desalted and concentrated in ZipTipC18 devices (Millipore).

**Optimized enrichment procedure for phosphopeptides.** HAP was performed in order to obtain an enriched fraction of phosphopeptides. HAP spin

down column was manufactured in our laboratory using BIO-GEL HTPP/sample ratio 2 : 1 (mg/ $\mu$ l). Ten milliliters of the reconstituted peptides mixture was dried in a vacuum centrifuge and resuspended in 100  $\mu$ l of loading buffer (TRIS 10 mM, EDTA, 1 mM pH 7). The peptides solution was loaded onto 20 mg of HAP that was previously packed with loading buffer. The HAP-bound peptides were incubated at room temperature for 15 min twice. After, the column was washed with loading buffer to remove unretained peptides. The phosphopeptides were eluted with 100  $\mu$ l of elution buffer (KCl 100 mM, TRIS 20 mM, EDTA 2 mM, pH 8). All fraction were dried in a vacuum centrifuge, resuspended in 100  $\mu$ l of 40% ACN/0.1%, desalted in reverse-phase Zip Tips.

**Protein identification by MALDI MS and MS/MS analysis:** Ten microliters of the all fractions was desalted using ZipTipC18 prior MS analysis. Peptides were eluted directly into 5  $\mu$ l of matrix solution (5 mg/ $\mu$ l R-cyano-4-hydroxycinnamic acid (CHCA) in 50% ACN, 0.1% v/v TFA) in order to maximize concentration of peptides in sample spot. Mass spectrometry analyses were performed using an 5800 MALDI-TOF-TOF Analyzer (AB SCIEX, Darmstadt, Germany) equipped with a neodymium: yttrium-aluminum-garnet laser (laser wavelength was 349 nm), in reflection positive-ion mode with a mass accuracy of 5 p.p.m. At least 4000 laser shots were typically accumulated with a laser pulse rate of 400 Hz in the MS mode, whereas in the MS/MS mode spectra up to 5000 laser shots were acquired and averaged with a pulse rate of 1000 Hz. MS/MS experiments were performed at a collision energy of 1 kV, ambient air was used as collision gas with medium pressure of 10<sup>-6</sup> Torr. After acquisition, spectra were handled using Data Explorer version 4.0. The mass data were processed to assign candidate peptides in the SwissProt database using the MASCOT search program. Peptide Mass Fingerprinting (PMF) interrogation identified (P05412), TRANSCRIPTION FACTOR AP-1 (PROTO-ONCOGENE C-JUN) (P39) (G0S7) using 34 *m/z* values, sequence coverage: 62%, (score 91). A mass tolerance of 50 p.p.m. was used and up to four missed pepsin cleavage was allowed.

## Conflict of Interest

The authors declare no conflict of interest

**Acknowledgements.** We thank Dr. Axel Behrens from providing c-Jun fl mice; Dr. Hans van Dam for the Jun2 reporter plasmid; Mrs Regine Sendtner for technical assistance in the mouse facilities and Mrs. Elke Spirk for lentiviral production. We thank Dr. Robert Blum and Professor Michael Sendtner for critical discussion of results. We are very thankful to Professor M Sendtner for having offered to our team laboratory space and the unlimited use of all facilities. Funding for this project was provided by the Deutsche Forschungsgemeinschaft (MU 2838/2-1); Associazione Italiana per la Ricerca sul Cancro (AIRC, 12849/2012), AIRC project Calabria 2011 and Fondazione Cassa di Risparmio di Calabria e Lucania.

- Hess J, Angel P, Schorpp-Kistner M. AP-1 subunits: quarrel and harmony among siblings. *J Cell Sci* 2004; **117**: 5965–5973.
- Shaulian E, Karin M. AP-1 in cell proliferation and survival. *Oncogene* 2001; **20**: 2390–2400.
- Eferl R, Wagner EF. AP-1: a double-edged sword in tumorigenesis. *Nat Rev Cancer* 2003; **3**: 859–868.
- Karin M, Gallagher E. From JNK to pay dirt: Jun Kinases, their Biochemistry, physiology and clinical importance. *IUBMB Life* 2005; **57**: 283–295.
- Davis RJ. Signal Transduction by the JNK Group of MAP Kinases. *Cell* 2000; **103**: 239–252.
- Dunn C, Wiltshire C, MacLaren A, Gillespie DAF. Molecular mechanism and biological functions of c-Jun N-terminal kinase signalling via the c-Jun transcription factor. *Cell Signa* 2002; **14**: 585–593.
- Weiss C, Schneider S, Wagner EF, Zhang X, Seto E, Bohmann D. JNK phosphorylation relieves HDAC3-dependent suppression of the transcriptional activity of c-Jun. *EMBO J* 2003; **22**: 3686–3695.
- Vinciguerra M, Esposito I, Salzano S, Madeo A, Nagel G, Maggolini M *et al*. Negative charged threonine 95 of c-Jun is essential for c-Jun N-terminal kinase-dependent phosphorylation of threonine 91/93 and stress-induced c-Jun biological activity. *Int J Biochem Cell Biol* 2008; **40**: 307–316.
- Papavassiliou AG, Treier M, Bohmann D. Intramolecular signal transduction in c-Jun. *Embo J* 1995; **14**: 2014–2019.
- Bannister AJ, Oehler T, Wilhelm D, Angel P, Kouzarides T. Stimulation of c-Jun activity by CBP: c-Jun residues Ser63/73 are required for CBP induced stimulation in vivo and CBP binding in vitro. *Oncogene* 1995; **11**: 2509–2514.

- Tsai LN, Ku TKS, Salib NK, Crowe DL. Extracellular signals regulate rapid coactivator recruitment at ap-1 sites by altered phosphorylation of both CREB binding protein and c-jun. *Mol Cell Biol* 2008; **28**: 4240–4250.
- Aguilera C, Nakagawa K, Sancho R, Chakraborty A, Hendrich B, Behrens A. c-Jun N-terminal phosphorylation antagonises recruitment of the Mbd3/NuRD repressor complex. *Nature* 2011; **469**: 231–235.
- Ogawa S, Lozach J, Jepsen K, Sawka-Verhelle D, Perissi V, Sasik R *et al*. A nuclear receptor corepressor transcriptional checkpoint controlling activator protein 1-dependent gene networks required for macrophage activation. *Proc Natl Acad Sci USA* 2004; **101**: 14461–14466.
- Morton S, Davis RJ, McLaren A, Cohen P. A reinvestigation of the multisite phosphorylation of the transcription factor c-Jun. *EMBO J* 2003; **22**: 3876–3886.
- Vinciguerra M, Vivacqua A, Fasanella G, Gallo A, Cuzzo C, Morano A *et al*. Differential phosphorylation of c-Jun and JunD in response to the epidermal growth factor is determined by the structure of MAPK targeting sequences. *J Biol Chem* 2004; **279**: 9634–9641.
- Hayakawa J, Mittal S, Wang Y, Korkmaz KS, Adamson E, English C *et al*. Identification of promoters bound by c-Jun/ATF2 during rapid large-scale gene activation following genotoxic stress. *Mol Cell* 2004; **16**: 521–535.
- Madeo A, Vinciguerra M, Lappano R, Galgani M, Gasperi-Campani A, Maggolini M *et al*. c-Jun activation is required for 4-hydroxytamoxifen-induced cell death in breast cancer cells. *Oncogene* 2009; **29**: 978–991.
- Bagowski CP, Besser J, Frey CR, Ferrell JE. The JNK Cascade as a Biochemical Switch in Mammalian Cells: Ultrasensitive and All-or-None Responses. *Curr Biol* 2003; **13**: 315–320.
- Raivich G, Behrens A. Role of the AP-1 transcription factor c-Jun in developing, adult and injured brain. *Prog Neurobiol* 2006; **78**: 347–363.
- Raivich G. c-Jun Expression, activation and function in neural cell death, inflammation and repair. *J Neurochem* 2008; **107**: 898–906.
- Waetzig V, Zhao Y, Herdegen T. The bright side of JNKs—multitalented mediators in neuronal sprouting, brain development and nerve fiber regeneration. *Prog Neurobiol* 2006; **80**: 84–97.
- Behrens A, Sibilina M, Wagner EF. Amino-terminal phosphorylation of c-Jun regulates stress-induced apoptosis and cellular proliferation. *Nat Genet* 1999; **21**: 326–329.
- Besirli CG, Wagner EF, Johnson EM. The limited role of NH2-terminal c-Jun phosphorylation in neuronal apoptosis: Identification of the nuclear pore complex as a potential target of the JNK pathway. *J Cell Biol* 2005; **170**: 401–411.
- Watson A, Eilers A, Lallemand D, Kyriakis J, Rubin LL, Ham J. Phosphorylation of c-Jun is necessary for apoptosis induced by survival signal withdrawal in cerebellar granule neurons. *J Neurosci* 1998; **18**: 751–762.
- Yuan Z, Gong S, Luo J, Zheng Z, Song B, Ma S *et al*. Opposing roles for ATF2 and c-Fos in c-Jun-mediated neuronal apoptosis. *Mol Cell Biol* 2009; **29**: 2431–2442.
- Dragunow M, Xu R, Walton M, Woodgate A-M, Lawlor P, MacGibbon GA *et al*. c-Jun promotes neurite outgrowth and survival in PC12 cells. *Mol Brain Res* 2000; **83**: 20–33.
- Leppa S, Saffrich R, Ansorge W, Bohmann D. Differential regulation of c-Jun by ERK and JNK during PC12 cell differentiation. *EMBO J* 1998; **17**: 4404–4413.
- Marek KW, Kurtz LM, Spitzer NC. c-Jun integrates calcium activity and tix3 expression to regulate neurotransmitter specification. *Nat Neurosci* 2010; **13**: 944–950.
- Albanito L, Reddy CE, Musti AM. c-Jun is essential for the induction of Il-1 $\beta$  gene expression in in vitro activated Bergmann glial cells. *Glia* 2011; **59**: 1879–1890.
- Haeusgen W, Boehm R, Zhao Y, Herdegen T, Waetzig V. Specific activities of individual c-Jun N-terminal kinases in the brain. *Neuroscience* 2009; **161**: 951–959.
- Ambacher KK, Pitzul KB, Karajgikar M, Hamilton A, Ferguson SS, Cregan SP. The JNK- and AKT/GSK3 $\beta$ - signaling pathways converge to regulate puma induction and neuronal apoptosis induced by trophic factor deprivation. *PLoS One* 2012; **7**: e46885.
- Hongisto V, Smeds N, Brecht S, Herdegen T, Courtney MJ, Coffey ET. Lithium blocks the c-Jun stress response and protects neurons via its action on glycogen synthase kinase 3. *Mol Cell Biol* 2003; **23**: 6027–6036.
- Coffey ET, Smicicene G, Hongisto V, Cao J, Brecht S, Herdegen T *et al*. c-Jun N-Terminal protein kinase (JNK) 2/3 is specifically activated by stress, mediating c-Jun activation, in the presence of constitutive JNK1 activity in cerebellar neurons. *J Neurosci* 2002; **22**: 4335–4345.
- Raivich G, Bohatschek Mo, Da Costa C, Iwata O, Galiano M, Hristova M *et al*. The AP-1 Transcription factor c-Jun is required for efficient axonal regeneration. *Neuron* 2004; **43**: 57–67.
- Napoli A, Aiello D, Di Donna L, Moschidis P, Sindona G. Vegetable proteomics: The detection of ole e 1 isoallergens by peptide matching of MALDI MS/MS Spectra of underivatized and dansylated glycopeptides. *J Proteome Res* 2008; **7**: 2723–2732.
- Hernandez P, Müller M, Appel RD. Automated protein identification by tandem mass spectrometry: issues and strategies. *Mass Spectrom Revs* 2006; **25**: 235–254.
- Nateri AS, Spencer-Dene B, Behrens A. Interaction of phosphorylated c-Jun with TCF4 regulates intestinal cancer development. *Nature* 2005; **437**: 281–285.
- Waetzig V, Herdegen T. Neurodegenerative and physiological actions of c-Jun N-terminal kinases in the mammalian brain. *Neurosci Lett* 2004; **361**: 64–67.
- Comalada M, Lloberas J, Celada A. MKP-1: A critical phosphatase in the biology of macrophages controlling the switch between proliferation and activation. *Eu J Immunol* 2012; **42**: 1938–1948.



40. Raman M, Chen W, Cobb MH. Differential regulation and properties of MAPKs. *Oncogene* 2007; **26**: 3100–3112.
41. Ventura J-J, Hübner A, Zhang C, Flavell RA, Shokat KM, Davis RJ. Chemical genetic analysis of the time course of signal transduction by JNK. *Mol Cell* 2006; **21**: 701–710.
42. Lu C, Zhu F, Cho Y-Y, Tang F, Zykova T, Ma W-y *et al*. Cell apoptosis: requirement of H2AX in DNA ladder formation, but not for the activation of caspase-3. *Mol Cell* 2006; **23**: 121–132.
43. Sluss HK, Davis RJ. H2AX is a target of the JNK signaling pathway that is required for apoptotic DNA fragmentation. *Mol Cell* 2006; **23**: 152–153.
44. Björklom B, Vainio JC, Hongisto V, Herdegen T, Courtney MJ, Coffey ET. All JNKs can kill, but nuclear localization is critical for neuronal death. *J Biol Chem* 2008; **283**: 19704–19713.
45. Sengupta Ghosh A, Wang B, Pozniak CD, Chen M, Watts RJ, Lewcock JW. DLK induces developmental neuronal degeneration via selective regulation of proapoptotic JNK activity. *J Cell Biol* 2011; **194**: 751–764.
46. Behrens A, Sibilia M, David JP, Mohle-Steinlein U, Tronche F, Schutz G *et al*. Impaired postnatal hepatocyte proliferation and liver regeneration in mice lacking c-jun in the liver. *Embo J* 2002; **21**: 1782–1790.
47. Tronche F, Kellendonk C, Kretz O, Gass P, Anlag K, Orban PC *et al*. Disruption of the glucocorticoid receptor gene in the nervous system results in reduced anxiety. *Nat Genet* 1999; **23**: 99–103.
48. Lois C, Hong EJ, Pease S, Brown EJ, Baltimore D. Germline transmission and tissue-specific expression of transgenes delivered by lentiviral vectors. *Science* 2002; **295**: 868–872.
49. Bender FP, Fischer M, Funk N, Orel N, Rethwilm A, Sendtner M. High-efficiency gene transfer into cultured embryonic motoneurons using recombinant lentiviruses. *Histochem Cell Biol* 2007; **127**: 439–448.
50. Morrison BE, Majdzadeh N, Zhang X, Lyles A, Bassel-Duby R, Olson EN *et al*. Neuroprotection by histone deacetylase-related protein. *Mol Cell Biol* 2006; **26**: 3550–3564.
51. Duppatla V, Gjorgjevikj M, Schmitz W, Kottmair M, Mueller TD, Sebald W. Enzymatic deglutathionylation to generate interleukin-4 cysteine muteins with free thiol. *Bioconjugate Chem* 2012; **23**: 1396–1405.
52. Napoli A, Athanassopoulos CM, Moschidis P, Aiello D, Di Donna L, Mazzotti F *et al*. Solid phase isobaric mass tag reagent for simultaneous protein identification and assay. *Anal Chem* 2010; **82**: 5552–5560.



**Cell Death and Disease is an open-access journal published by Nature Publishing Group. This work is licensed under a Creative Commons Attribution-NonCommercial-NoDerivs 3.0 Unported License. To view a copy of this license, visit <http://creativecommons.org/licenses/by-nc-nd/3.0/>**

Supplementary Information accompanies this paper on Cell Death and Disease website (<http://www.nature.com/cddis>)